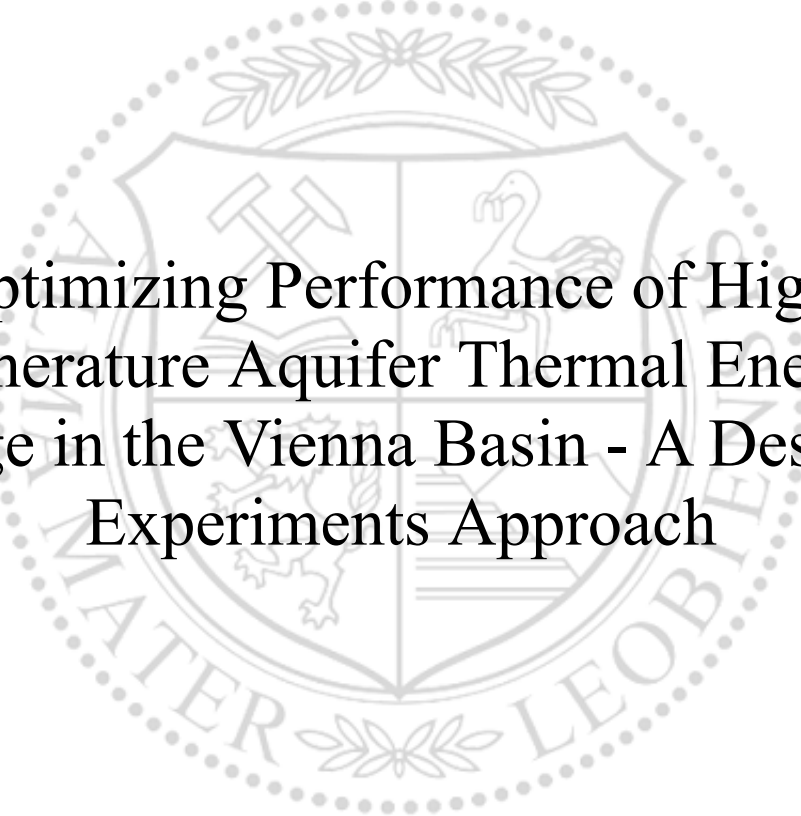




Chair of Geoenergy Production Engineering

Master's Thesis



Optimizing Performance of High-Temperature Aquifer Thermal Energy Storage in the Vienna Basin - A Design of Experiments Approach

Philipp Werkl, BSc

May 2024



**EIDESSTÄTLICHE ERKLÄRUNG**

Ich erkläre an Eides statt, dass ich diese Arbeit selbstständig verfasst, andere als die angegebenen Quellen und Hilfsmittel nicht benutzt, den Einsatz von generativen Methoden und Modellen der künstlichen Intelligenz vollständig und wahrheitsgetreu ausgewiesen habe, und mich auch sonst keiner unerlaubten Hilfsmittel bedient habe.

Ich erkläre, dass ich den Satzungsteil „Gute wissenschaftliche Praxis“ der Montanuniversität Leoben gelesen, verstanden und befolgt habe.

Weiters erkläre ich, dass die elektronische und gedruckte Version der eingereichten wissenschaftlichen Abschlussarbeit formal und inhaltlich identisch sind.

Datum 13.05.2024

---

Unterschrift Verfasser/in  
Philipp Werkl

Philipp Werkl, B.Sc.  
Master Thesis 2024  
Geoenery Engineering

# Optimizing Performance of High-Temperature Aquifer Thermal Energy Storage in the Vienna Basin – A Design of Experiments Approach

Supervisor: Yoshioka Keita; Univ.-Prof. PhD  
Co-supervisor: Albishini Ramzy; Dipl.-Ing.

Chair of Petroleum and Geothermal Energy  
Recovery

*Dedicated to my family and friends.*

## **Acknowledgments**

I hereby want to acknowledge my family and friends for always supporting me, not only during the fun and exciting times but especially during hard times. I also want to extend my university colleagues gratitude, who helped me get through these last years with an emphasis on the people involved in guiding me through the final step, my thesis.

# Abstract

This thesis is about the design and optimization of a High-Temperature Aquifer Thermal Energy Storage (HT-ATES) system in the Vienna Basin, with a focus on the aquifer component. There are numerous parameters that influence the thermal recovery efficiency (R) of ATES, one main characteristic for the successful implementation of this kind of underground thermal energy storage (UTES). Therefore, the objective of this thesis is to determine the most influencing parameters and find the optimal combination of these to maximize the efficiency. To investigate the impact, assumptions are made on parameters and their respective range in agreement with a local geologist and numerical simulations are conducted to evaluate their influence on the performance of the aquifer. Ultimately, a design of experiments (DoE) approach is used to obtain a thorough analysis of the results. By analyzing the simulations, statements about the pressure and temperature distribution within an aquifer are made and the combination of parameters within the specified range that yield the highest performance are determined.

## Zusammenfassung

Diese Arbeit befasst sich mit der Auslegung und Optimierung eines Hochtemperatur-Aquifer-Thermalspeichersystems (HT-ATES) im Wiener Becken, wobei der Schwerpunkt auf dem Aquifer liegt. Es gibt zahlreiche Parameter, die die thermische Rückgewinnungseffizienz ( $R$ ) von ATES beeinflussen, ein Hauptmerkmal für die erfolgreiche Implementierung dieser Art von unterirdischen thermischen Energiespeichern (UTES). Ziel dieser Arbeit ist es daher, die einflussreichsten Parameter zu bestimmen und die optimale Kombination dieser Parameter zu finden, um die Effizienz zu maximieren. Um die Auswirkungen zu untersuchen, werden in Absprache mit einem lokalen Geologen Annahmen zu den Parametern und ihrer jeweiligen Bandbreite getroffen und numerische Simulationen durchgeführt, um ihren Einfluss auf die Leistung des Aquifers zu bewerten. Letztendlich wird ein design of experiments (DoE) Ansatz verwendet, um eine gründliche Analyse der Ergebnisse zu erhalten. Durch die Analyse der Simulationen werden Aussagen über die Druck- und Temperaturverteilung innerhalb eines Aquifers getroffen und die Kombination von Parametern innerhalb des vorgegebenen Bereichs ermittelt, die die höchste Leistung erbringen.





# Table of Contents

The table of contents below is automatically generated by Word. To update this after revisions, right-click in the table and choose “*Update Field*” for the entire table.

Chapter 1.....	11
Chapter 2.....	13
2.1    Underground Thermal Energy Storage .....	13
2.2    Aquifer Thermal Energy Storage .....	16
2.3    Aquifer Characteristics relevant to ATES systems .....	21
2.4    Design of Experiments .....	24
Chapter 3.....	28
3.1    Finite Element Flow Simulation .....	28
3.2    Design of Experiments Approach .....	33
Chapter 4.....	35
Chapter 5.....	41
References .....	43
Appendix .....	47



# Chapter 1

## Introduction

Enhancing energy efficiency in buildings remains a significant area for improvement at a global scale. Not only for existing buildings and their heating and cooling systems in developed countries but also for the increasing urban population in developing countries high performance standards for efficient heating and cooling present a huge opportunity to decrease carbon emissions in this sector. The end-use worldwide accounts for more than 40 EJ, the equivalent of more than 11 PWh per year. (*World Energy Outlook 2023*, n.d.) At the latest Conference of the Parties (COP) in 2023 the member states declared energy efficiency as the “first fuel” in the fight against climate change. A pledge has been made by the member states to double the current global annual rate of energy efficiency improvements per year until 2030. (*COP28*, n.d.) Thermal Energy Storage (TES) is a technology that may be used to balance discrepancies between the supply and demand of energy while at the same facilitating more efficient utilization of industrial waste heat or cold, as well as renewable energy sources like solar. (Lu et al., 2019) One of the most promising TES concepts is the use of aquifers as a heat storage medium, to seasonally store heat which would otherwise be considered as excessive or waste. (Mangold et al., 2004) As the energy is stored below the surface, this system is classified as an underground thermal energy storage (UTES) which has the benefit of a small footprint on the surface. Due to its high storage capacities, it is commonly used in seasonal, large-scale operations. Furthermore, ATES can be categorized into low-temperature and high-temperature systems, whereby different parameters need to be considered and the temperature range they operate in make them more suited for one or another application. (Kleyböcker & Bloemendal, 2020) While there are more than a couple of thousands low-temperature systems in operation, there are only a handful HT-ATES constructed and in use which makes it more complex regarding meaningful interpretation of the results and findings. Therefore, this thesis is dedicated to HT-ATES, more specifically to the pre-investigative phase of the project lifecycle.

While there are many components in an ATEs system that need to be thoroughly designed and selected, the focus of this thesis is placed on the aquifer itself. Through literature review the relevant parameters and concepts that influence the performance of the storage system are identified and put into context. A numerical model is used to build and simulate a conceptual aquifer to create a base case with a set of properties that is based on literature and adjusted to potential values in the Vienna Basin by a geologist that has knowledge and insight over the geological conditions in the area. As these numerous conditions are tied to significant variations and high uncertainty, the parameters that influence the thermal recovery efficiency are investigated to determine the extent of their impact. The parameters with high significance are further investigated in a fractional factorial design to identify the optimal combination of parameters that maximize the thermal recovery efficiency.

# Chapter 2

## Literature Review

### 2.1 Underground Thermal Energy Storage

UTES methods represent an opportunity to efficiently store and utilize thermal energy. There are various systems with its associated advantages and disadvantages, and it depends on various factors to determine which one is best suited for an individual application. (Kallesøe & Vangkilde-Pedersen, 2019) The selection of the system that fits the circumstances best depends on storage capacity and efficiency, system boundary conditions like integration into a heating network, temperature requirements, legal restrictions, (hydro-) geological situation and more. (Schmidt et al., 2018) High storage capacities and efficiencies make UTES a sensible thermal energy storage method and therefore a particularly well choice for long-term TES. (Fleuchaus et al., 2018)

Apart from ATES which will be further classified as High-Temperature ATES (HT-ATES) and Low-Temperature ATES (LT-ATES) and is described in more detail in the following subchapters, three alternatives are presented briefly here to give an overview of UTES in general. These additional thermal energy storage methods include borehole thermal energy storage (BTES), pit thermal energy storage (PTES), and mine thermal energy storage (MTES).

BTES consists of many closed loop borehole heat exchangers (BHE) and can utilize a large volume of underground soil or rock by efficient placement of these boreholes in an array. Its underlying effect is the utilization of the natural heat capacity, and therefore the storage of heat in the surrounding subsurface where, in contrast to ATES, a closed loop system mode is applied. The working principle is to cyclically heat up and cool down the storage volume by circulating a working fluid in pipes within the borehole which then transfer their heat through the surrounding sealing grout into the formation. An effective use of BTES can be achieved by linking the system to renewable energy sources that produce excess heat, such as solar thermal,

combined heat and power (CHP), or heat pumps. Technical limitations to this kind of UTES are 20-200 m depth and up to 90°C storage temperature, while the boreholes are usually 2-5 m apart from each other. The recovery efficiency is often lower than expected and is in the range of 45% to 60%, with industrial excess heat and solar as their heat source. This may be caused by various factors like among others, inadequate storage design, greater than expected heat losses, or assuming parameters in the modelling that do not represent the appropriate local conditions. (Kallesøe & Vangkilde-Pedersen, 2019)

In Figure 1 the conceptual setup of BTES is visualized.

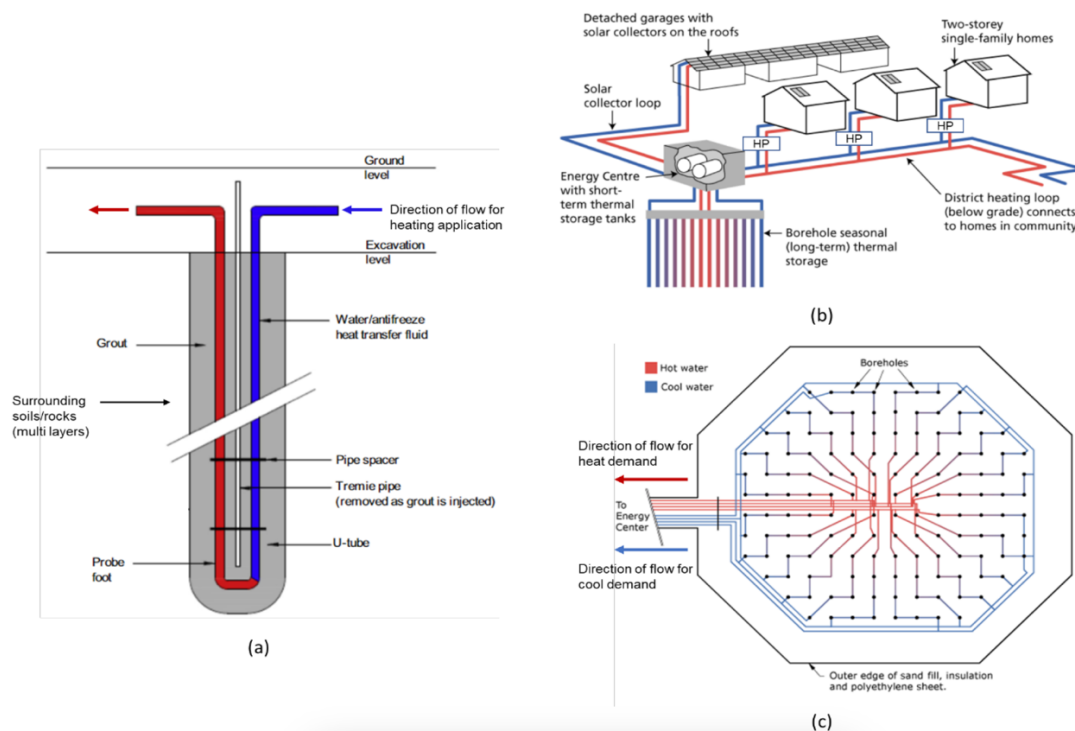


Figure 1: BTES conceptual model. (a) cross-sectional view of the system (b) model of the whole system in combination with DHN (c) borehole array from a bird's-eye view (Gao et al., 2023)

PTES in comparison to ATEs has a simple working principle and consists of a large basin which is excavated with few additional components. The pit is typically insulated from all six dimensions to restrict heat losses from the system by polymer liners and a lid, where the sides and the bottom planes are frequently made of concrete. Its flexibility in charging and discharging, and the usage of water which represents an optimal storage medium due to its high thermal heat capacity make this system prone to be used in combination with district heating networks (DHNs). However, PTES is very space demanding which makes it occasionally hard to implement into urban areas. In terms of storage efficiency, the data shows a large discrepancy. This showcases the importance of a thorough workflow from the beginning, e.g., the planning phase until the operation of the system itself. Two plant examples which are both

located in Denmark in terms of efficiency are 89.5% and 50.3%. Their storage volumes are 60,000 m<sup>3</sup> and 122,000 m<sup>3</sup>, respectively. (Kallesøe & Vangkilde-Pedersen, 2019)

In Figure 2 a real photograph and the conceptual setup of PTES is visualized.

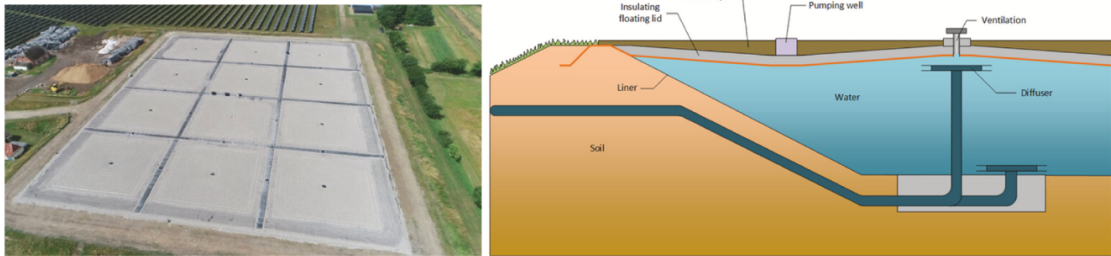


Figure 2: PTES. Real image in bird's-eye view and a conceptual cross-sectional view (Xiang et al., 2022)

Direct use of mine water utilizes a low-temperature energy source using abandoned and flooded mines and a few plants already exist at this point. However, the possibility of using mines that are no longer in use for MTES is a concept that has not been explored in the extend that relevant data can be presented. With the current state of knowledge, the requirements for this type of thermal storage, the requirements to effectively utilize old mines for this application are large mine water volume, reliability, cost effectiveness and the possibility to integrate the system into urban areas. Its conceptual idea is similar to the prior mentioned thermal energy storage methods, where excess heat that is seasonally unutilized during summer is used to heat up the storage medium. During winter the gained heat within the MTES is then used for heating purposes. (Kallesøe & Vangkilde-Pedersen, 2019)

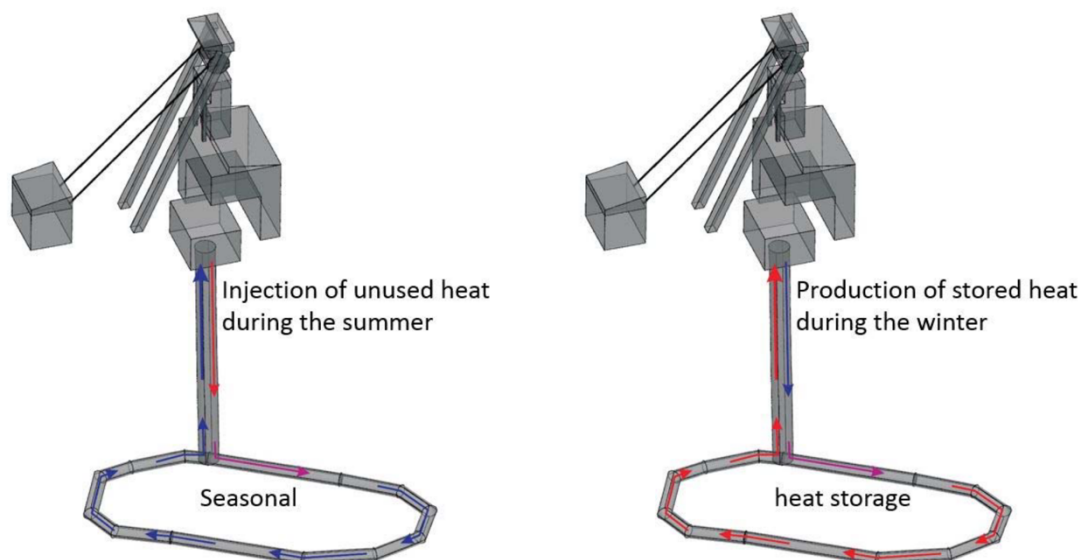


Figure 3: MTES. Operating cycle in summer and winter (Kallesøe & Vangkilde-Pedersen, 2019)

## 2.2 Aquifer Thermal Energy Storage

ATES systems use an aquifer's groundwater as a heat carrier which makes it a so-called open-loop system. The systems either consists of a simple well doublet (One injection and one production well), or more pairs of wells that simultaneously produce and inject from and into an underground formation. Considering a temperature difference in the injection and production volume of the fluid, this allows to alter the temperature of the subsurface and hence extract or store thermal energy in a seasonal manner. (Aydin Ertuğrul et al., 2018) Among other UTES concepts, ATES is considered to have the highest storage capacities which makes it particularly suitable for large scale operations. As it is an open-loop system, the requirements are more stringent compared to closed-loop systems, as favorable conditions like high permeability, low groundwater flow, and geochemical conditions that prevent clogging and well corrosion are all prerequisites for an efficient system. (Fleuchaus et al., 2018) Their integration into DHNs with an external heat supply by e.g. solar collectors poses a promising way to enhance the efficiency of energy systems. In addition, if the outlet temperature of the ATES plant is insufficient, heat pumps can be used to boost temperatures to the level the DHN or other applications require to operate. (Kallesøe & Vangkilde-Pedersen, 2019)

The principal idea of ATES dates to the 1960s in Shanghai. It was observed, that injected surface water temperature can hold its temperature over several months and thus at the time, the concept was used to store cold from the winter months to utilize it for industrial cooling in summer. After this observation, the number of wells in operation increased rapidly and peaked in China during the 1980s. During the 1970s, presumably connected to the oil crisis that took place at the time, research and development (R&D) into ATES was intensified in both, North America, and Europe. 1978 marked an important milestone in the history of this TES, the International Energy Agency (IEA) established an agreement on Energy Conservation through Energy Storage (ECES). Its target was to support energy storage system development and within this framework, significant measurements on how to prevent scaling, the potential environmental impact of ATES, as well as how to overcome thermohydraulic-related problems like thermal breakthrough, buoyancy flow, unbalance between stored heat and cold were developed. The insight that was achieved was that careful pre-investigation and a well-planned operational design are mandatory for the successful implementation of systems. (Fleuchaus et al., 2018)

In Figure 4 the previously addressed achievements are indicated on a timeline. Additionally, further pioneering successes are indicated.



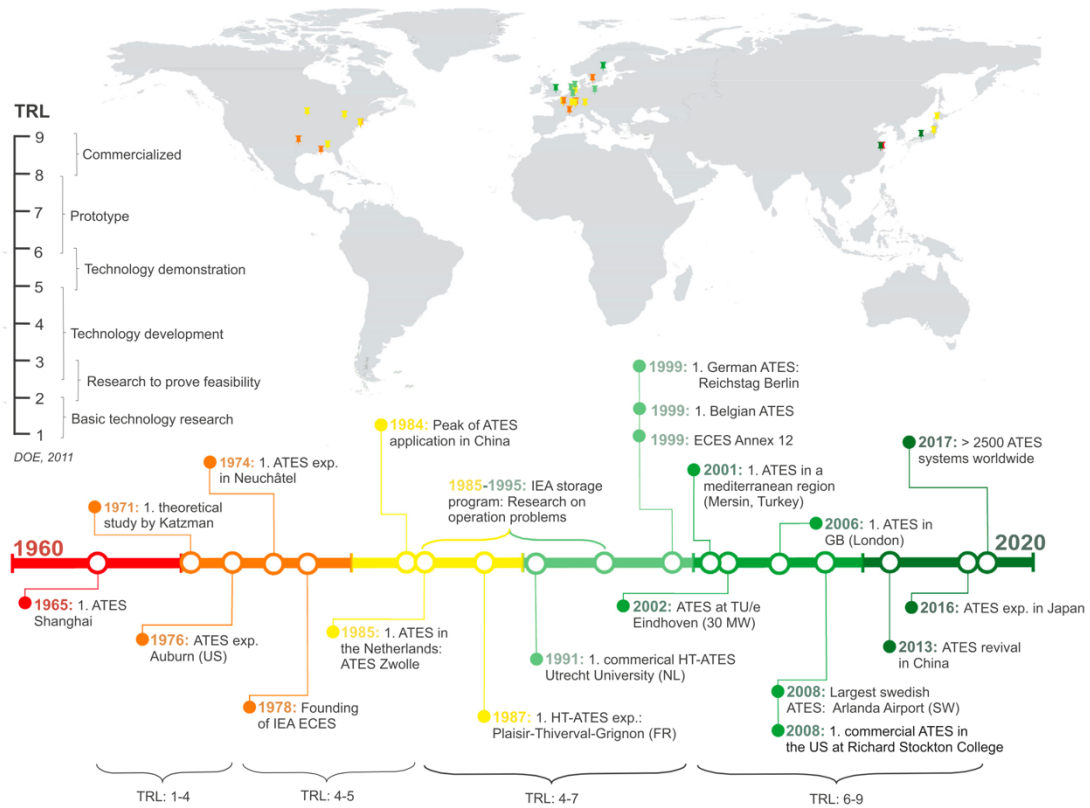


Figure 4: Achievements in the history of ATES projects from 1960 until 2020 (Fleuchaus et al., 2018)

As of 2018, around 2800 ATES projects, accounting for more than 2.5 TWh heat and cold produced per year, have been successfully implemented worldwide, of which are more than 99% LT-ATES. This is mostly the case because these systems, compared to HT-ATES encountered less problems and the focus was shifted to establishing an implementation into the energy markets of a few countries. The great discrepancy in the spatial distribution is due to several market barriers such as legislative and socio-economic reasons. (Fleuchaus et al., 2018)

The adoption of ATES throughout the globe is mainly promoted by governments that follow emission reduction targets and/or energy-saving pledges. Even if the respective government follows that strategy, there are two factors that limit their commitment to pursue this technology. First, high initial costs deter decision-makers to invest. However, in cases with accurate planning and thorough operation ATES brings more economic benefit than fossil fuel applications. Operational problems and failures are the second factor to raise uncertainty. With improving technology and lessons learned from previous projects, this reason not to implement ATES attenuates, too. (Lu et al., 2019) conducted a study, assessing the global potential for ATES. They integrated suitability, vulnerability, and sustainability indicators into their work, while also including different decision makers' attitudes. By setting the three properties to neutral in regard to the behavioral pattern of judgement, meaning that the decisions are neither optimistic, nor pessimistic, the global potential score results in Figure 5 can be obtained.

Considering medium results corresponding to a score higher than 10, the proportion of potential surface are around the globe are 59% in Oceania, 50% in South America, 48% in Europe, 21% in North America, 20% in Asia, and 16% in Africa.

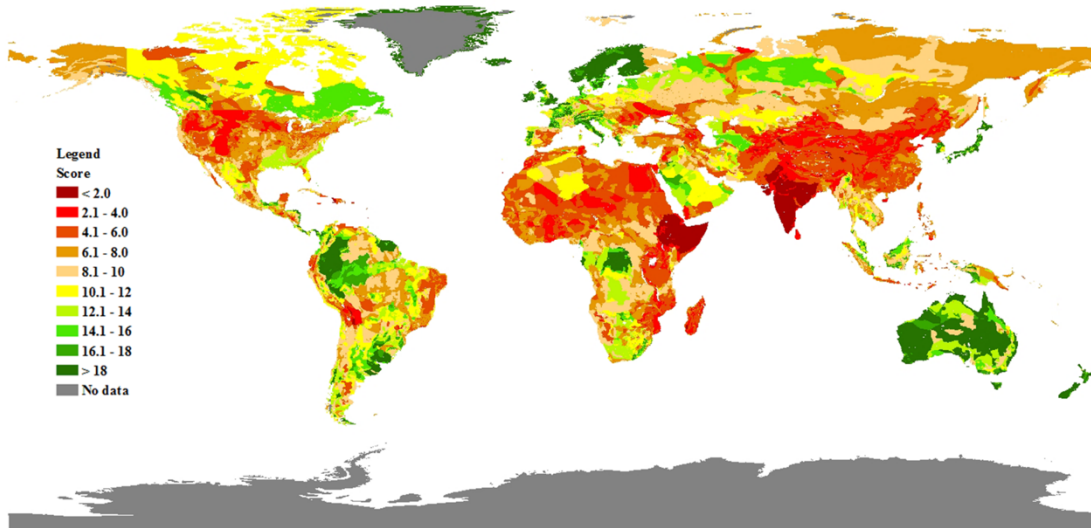


Figure 5: Global potential of ATES on a global scale (Lu et al., 2019)

Several temperature ranges can be found to distinguish, whether a system is considered LT-ATES or HT-ATES. According to (Kallesøe & Vangkilde-Pedersen, 2019), high-temperature design requires an injection temperature of  $>60^{\circ}\text{C}$ , low-temperature systems are described by  $<30^{\circ}\text{C}$ . In between, they describe systems as medium-temperature ATES (MT-ATES). (Gao et al., 2017) denote HT-ATES systems in the case of  $>50^{\circ}\text{C}$  injection temperature and (Nitschke et al., n.d.) classify the high-temperature operation above  $100^{\circ}\text{C}$ . If the notation of (Kallesøe & Vangkilde-Pedersen, 2019) is followed, there have been only five operating HT-ATES worldwide in 2018. This small number is the reason why there is not plenty of literature on already existing projects, yet.

Whereas HT-ATES usually require deep geological formations, LT-ATES operations take place in shallower subsurface formations, more specifically in the upper few hundred meters of the surface. (Kallesøe & Vangkilde-Pedersen, 2019) The maximum temperature difference that is allowed by regulations within these shallow aquifers is restricted to a few tens of degrees in most countries. (Nielsen & Vangkilde-Pedersen, 2019)

In comparison to HT-ATES, lower thermal losses and density driven groundwater flow in the subsurface occur due to a smaller difference in temperature of the injected fluid and the surrounding groundwater. Also, usually there is no complex water treatment required and the specific material requirements for e.g. pumps are less significant. The downside of LT-ATES is its fewer possible applications, due to a lower temperature of the recovered heat. (Nielsen & Vangkilde-Pedersen, 2019)

The heat source for HT systems varies depending on the surrounding conditions. The most prominent are power plants, waste incineration plants, CHP plants, as well as solar thermal and residual heat from industry. Its large-scale storage application represents large potential to integrate the storage into DHNs, or geothermal energy systems. To achieve economic surplus and be competitive at the energy market, the external heat must be available at low cost to be competitive at the energy market. Among this pre-condition, there are further potential barriers that make this kind of energy storage somewhat complex to implement. Present regulatory aspects for the deployment of HT-ATES are sophisticated, permit procedures often represent themselves as uncertain, expensive and over a long time. Several regulations, e.g. including mining, construction, and water acts, as well as environmental issues must be considered to eliminate concerns for stakeholders and be consistent with the law in the area of interest. The environmental assessment should primarily focus on the following:

- Leakage prevention to surrounding or neighboring groundwater systems, especially shallow groundwater systems or the surface
- Preventing thermal impact on upper areas, especially these with drinking water interests, as well as other ATES or geothermal application in the vicinity
- Preventing unexpected microbiological, as well as hydro- and geochemical challenges in the storage system

(Nielsen & Vangkilde-Pedersen, 2019)

As mentioned before, there is only limited experience in the development and utilization of HT-ATES. Therefore, the design is primarily based on combined experience from deep geothermal systems and ATES systems with lower temperature. By realizing projects with high-temperature injection and storage in the future, the learning curve is expected to be steep, and the findings must be revised and implemented to achieve continuous improvement. (Nielsen & Vangkilde-Pedersen, 2019)

The timeline for an HT-ATES project can roughly be divided into four phases. The first one is the pre-investigation phase that includes a general feasibility study, risk analysis and system modelling. The second step consist of the actual construction of the system with the drilling process, the well configuration including design and material selection. This is followed by the system integration and lastly operations feedback, where monitoring, maintenance and the actual efficiency is compared to the simulated efficiency. Furthermore, water treatment and environmental issues must be closely watched to be in accordance with legal requirements. (Kallesøe & Vangkilde-Pedersen, 2019) As this thesis mainly focuses on the pre-investigation phase, more specifically on the numerical modelling of the aquifer, more focus is put on this first step of the project lifecycle. In HT-ATES, the key prerequisite for the successful

implementation are geological conditions. An aquifer with beneficial properties and dimensions is essential to the efficient operation. Geological screening is the key tool to make first assumptions on the suitability of an aquifer and depending on the availability of data for a specific area, these can be made with higher or lower accuracy. To take into account the risks associated with inaccurate data, the sensitivity of the system caused by different geological parameters is investigated.

The well configuration usually consists of a well doublet, while the number of doublets can increase, if more capacity and higher flowrates are required. A popular setup of a system containing more than two wells is the star-shaped configuration, which is depicted in Figure 6. On the upper left corner, a simple well doublet is shown, and its temperature iso-lines are compared to three different well configurations using the star-shaped setup. The hot wells are located in the middle of the system, while a ring of cold wells is surrounding them, capturing heat from the centered injection. By optimizing the well locations according to this type, the efficiency can be increased by up to 10%. (Nielsen & Vangkilde-Pedersen, 2019)

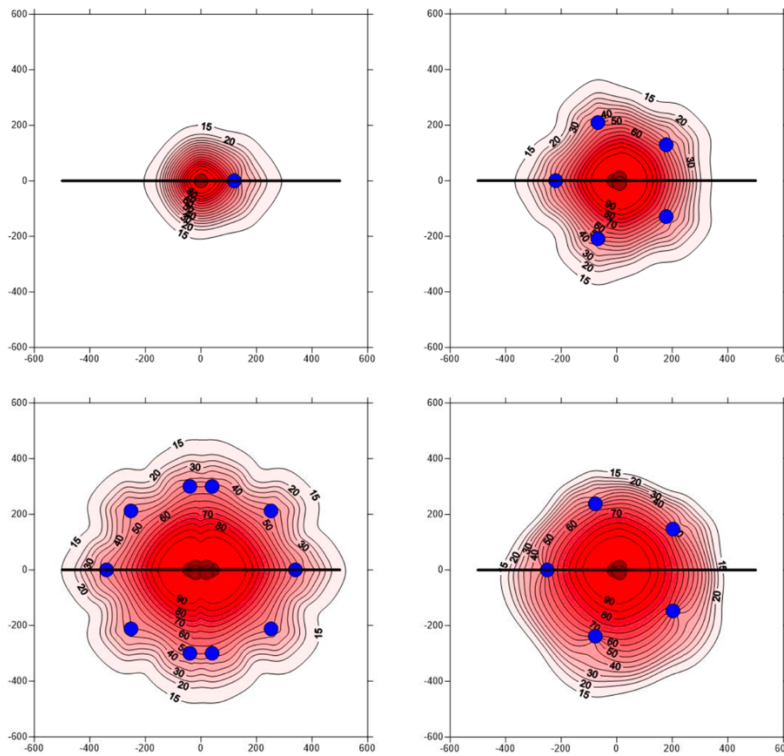


Figure 6: Well doublet and star-shaped configuration (Nielsen & Vangkilde-Pedersen, 2019)

The recovery efficiency of ATEs systems is defined by (Sheldon et al., 2021) in the following formula:

$$R = \frac{\overline{h_p} - h_{amb}}{h_i - h_{amb}} = \frac{\overline{T_p} - T_{amb}}{T_i - T_{amb}}$$

$T_{amb}$  being the ambient aquifer temperature,  $T_i$  the injection temperature and  $\overline{T_p}$  the average produced temperature.

## 2.3 Aquifer Characteristics relevant to ATEs systems

To understand the transport and thermal behavior of saturated porous media, fundamental flow dynamics, thermodynamic properties, and heat transfer mechanisms are essential. The most relevant parameters and underlying principles are indicated, and basic mathematical expressions are put into context in the following subchapters. In Table 1 an overview of the relevant parameters and properties in HT-ATES are listed. Please note, that a focus is put on the thermal properties in this thesis and therefore more information is provided on this.

<b>Geological and Hydrogeological Parameters</b>	<b>Hydrological Parameters</b>	<b>Thermal Properties</b>	<b>Geochemical properties</b>
Aquifer dimensions	Regional groundwater flow	Temperature and thermal gradient	Chemical composition
Aquifer heterogeneity	Hydraulic gradient and pressure	Thermal conductivity	pH value of groundwater
Aquifer permeability	Hydraulic conductivity/transmissivity	Heat capacity	Dissolved gases
Aquifer porosity	Specific storage	Thermal diffusivity	Density and viscosity
Aquifer anisotropy	Fracture network		Isotopes
Characteristics of confining layers	Well connectivity		Eh, TDS, TSS

*Table 1: Relevant aquifer parameters in ATEs (Kallesøe & Vangkilde-Pedersen, 2019)*

As indicated before identifying the geological conditions in the pre-investigative phase is crucial to assess the potential of an ATEs subsurface system. Understanding the geological characteristics of the aquifer helps to describe the suitability of a location, ensuring storage capacity and retrieval efficiency, where the aquifer dimensions in combination with the aquifer porosity provide information about the potential storage volume. Hydrogeological assessments provide insights into the movement and availability of groundwater. The ability of a material to allow fluid flow is described by permeability, or intrinsic permeability which only takes the

structure of the aquifer matrix into account. (García Gil et al., 2022) According to (Birdsell et al., 2021) it is likely that some intermediate permeability is favorable in ATES systems, as too low permeability hinders the propagation of injected water into the formation, while too excessive permeability can result in significant heat loss due to advection. Apart from the efficiency of the system, hydro-mechanical issues might be raised because of too high pressures around the injection well in case the fluid flow is restricted. The directional dependence of the aquifer's hydraulic properties, like the before-mentioned permeability is called anisotropy which is typical for fine-grained sediments. In specific cases, anisotropy also influences thermal properties where the alignment of crystal axes or fractures induces this phenomenon. (García Gil et al., 2022) The impact of thickness, permeability, and porosity on the nominal discharge capacity of the system is shown by (Daniilidis et al., 2022). Their results indicated that a higher permeability and a thicker aquifer both highly increase the discharge capacity of the system and simultaneously to a decrease of levelized cost of heat (LCOH). The relationship of changing the parameters in their range behaves linearly which is also applies to the change in porosity of the aquifer. However, changing the porosity neither has an influence on the LCOH, nor the nominal discharge capacity. Heterogeneity, being uneven changes and distributions of internal properties of the aquifer is considered to have a significant effect on the thermal efficiency, especially caused by dispersion that seriously impacts the thermal signature extent and shape within the system.

Hydrological parameters in the context of HT-ATES are essential for optimizing efficiency, sustainability, and safety of such systems. Understanding their impact on the performance and viability of the storage enables accurate prediction and ensures effective utilization of heat storage. Typically, a hydraulic gradient results in increased groundwater flow which impacts the displacement of stored volume in the ATES system. Depending on the magnitude, thermal losses occur by displacing hot injected water around the hot well of the doublet resulting in a decrease of the thermal recovery efficiency. (Bloemendal & Hartog, 2018) Hydraulic conductivity determines the flow path of water within the aquifer and especially vertical conductivity and its heterogeneity can influence the effectiveness of storage system. Especially in aquifers that are not confined, this can lead to mixing of different groundwater types, too which leads to a change in the composition of the water. (Possemiers et al., 2014) Specific storage that describes the ability or capacity of an aquifer to absorb and release water within the storage is another crucial property of ATES. Though there is no clear relationship of this parameter to the hydraulic conductivity, a positive correlation exists for some types of rocks. With an increase in porosity, the specific storage correlates positively, too. To evaluate the specific storage onsite, pumping test data are a tool that is frequently used and studied. (Kuang et al., 2020)

To reach high thermal recovery efficiency, thermal parameters of the subsurface formation must be considered. By examining the relevant properties, accurate prediction, and control of heat transfer processes during storage and retrieval phases can be made.

Thermal conductivity is an intrinsic material property that describes the ability of a substance to conduct heat. It measures how well a material can transfer heat through conduction, being the process by which heat is transferred within a material or between different materials in direct contact. A higher thermal conductivity indicates that a material is more effective in its ability to conduct heat. (García Gil et al., 2022) Heat capacity is a parameter that describes how much heat is required to change the temperature of a substance's mass (specific) or volume (volumetric) by a certain amount. Depending on the case, it is more useful to either use the specific or the volumetric heat capacity, while taking into account the density of both, the formation and the fluid filling up the pores. (García Gil et al., 2022) Thermal diffusivity describes how quickly a substance can conduct heat relative to how quickly it can undergo a change in temperature or simply its ability to store heat. A material with a higher thermal diffusivity exhibits a more pronounced reaction to temperature changes, leading to a swifter propagation of temperature perturbations within the material. (García Gil et al., 2022)

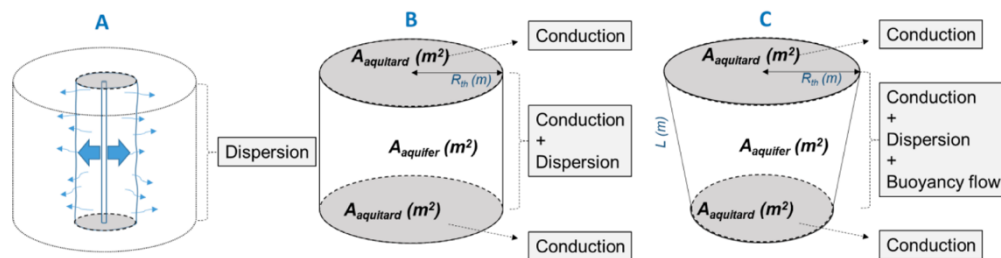


Figure 7: Heat losses in HT-ATES (Beernink et al., 2024)

The three processes that result in heat losses are illustrated in the figure above. These include conduction, dispersion and buoyancy driven flow. Conduction, that is present along the whole surface of a heat plume results in heat losses to the outer boundaries of the aquifer and the impermeable formations above and below, is the dominant factor for heat losses in LT-ATES. On the contrary, in HT-ATES the heat losses that are caused by natural convection due to density differences induced by temperature differences of stored and ambient aquifer water, becomes more important. (Beernink et al., 2024)

The performance and integrity of LT-ATES and HT-ATES can be significantly impacted by geochemical processes, resulting from different parameters within the system. Potential risks are corrosion, mineral precipitation, or groundwater contamination, which not only compromises the system efficiency but also raise concerns for potential environmental hazards. In high-temperature systems, larger temperature differences in formation, injection, and

production temperature occur which leads to an increased perturbation of the geochemical properties of the aquifer. This phenomenon, however, does not only impact the subsurface installation itself but also leads to an increased scaling potential (major scaling phases include e.g., calcite) at surface facilities. (Nitschke et al., n.d.) Chemical and microbial rates are highly significant in regions where temperatures increase, as they follow an exponential increase. The chemical equilibria and rate constants need to be assessed to get information about potential gas clogging and carbonate precipitation, which is caused by CO<sub>2</sub> degassing, that both lead to operational issues to the system. At LT-ATES sites, reaction kinetics and mineral equilibria have a minor effect in thermally balanced systems as the temperature differences are low, compared to deeper and warmer systems. To keep the impact on microbiological and chemistry of the shallow regions low and therefore protect the public water supply, the Netherlands introduced a policy to prevent injection temperatures above 25 – 30°C in shallow regions. In these regions, caution in mixing of stratified groundwater from various depths is of high importance is required to keep up the groundwater quality. (Hartog et al., 2013)

## **2.4 Design of Experiments**

Design of experiments (DOE) was primarily invented for agricultural purposes in the 1920s. Nowadays, it is widely used and applied in science, industry and computer simulation models and gives definitive conclusions from large amounts of data while minimizing the required resources like computational time. (Telford, 2007) Including a series of applied statistics tools, a systematically categorized and quantified causal relationship between variables and outputs in the studied process can be made to find an optimized configuration. While there are many different approaches on how to conduct DOE, the series of steps are equal in their approach: Planning, experiment execution and the analysis of the output data using statistical methods to reach valid conclusions. In the beginning of the workflow, the process needs to be selected and an investigation problem defined. Then, based on the performance indicator, also called response variable, the objectives are ascertained which is typically a quantitative measure, e.g. the thermal recovery efficiency. The parameters that are investigated to influence the system performance, called factors are stated and discretized accordingly and a suitable array or matrix for the simulation runs is created. After this is set up, the performance of the experiment in accordance with the collected data is analyzed and the results are interpreted. (Jankovic et al., 2021)

One important concept within DOE is the factorial experimental design. Its goal is to systematically explore the impacts of multiple factors by simultaneously manipulating them, as opposed to altering one factor independently at a time. This allows for estimation of individual



factor sensitivities as well as the interactions between two or more factors. (Telford, 2007) A factorial experiment that represents all conceivable combinations of the selected factors and their respective levels is referred to as full factorial design (FFD). The comprehensive nature of FFD renders its outcomes valuable benchmarks, as it covers all possible combinations of the input data and therefore provides the most thorough insight into the behavior of the system. This leads to a total number of runs that equals  $n^k$ , with  $n$  being the number of levels and  $k$  denoting the sum of the factors investigated. With an increasing number of factors and levels, the magnitude of experimental runs escalates significantly. In conventional experiments, this escalation entails considerable expenses, numerical simulations face the challenge of extremely long computational times. (Jankovic et al., 2021) This issue leads to the dilemma where computational or monetary resources compete with informative value of the experiments. In cases where it is not feasible or desirable to conduct a full factorial design which assesses all factors individually as well as their joint effects, identifying critical factors on which the further analysis focuses is an appropriate workflow. This step is called screening and various types exist to perform it, whole each of them has its advantages and disadvantages. (Gunst & Mason, 2009)

Figure 8 gives an overview of the main DOEs that are outlined in the following section, all assuming an experiment with three factors (A, B, C) and five levels (a, b, c, d, e). The full factorial design that is illustrated in the bottom right corner is compared in this figure in terms of which possible combinations of variables are applied in the workflow to different fractional factorial design methods.

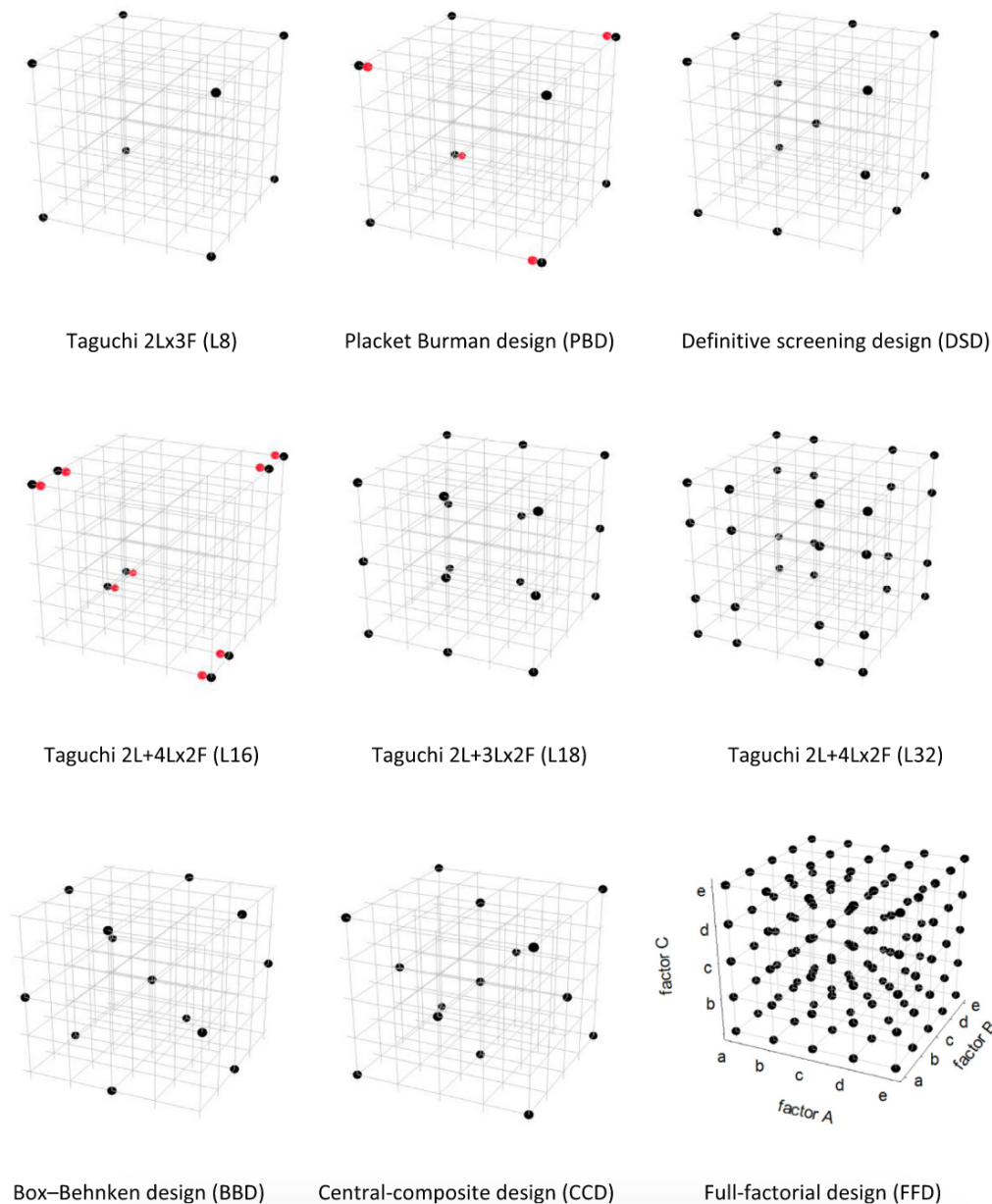


Figure 8: Various DoE for a three factor model on five levels (Jankovic et al., 2021)

Taguchi design (TD) gained widespread use in science and industry due to its practicality, even though the scientific community is hesitant. Its strength found in a minimized number of experimental runs needed, with an effective orthogonal matrix with balanced levels of factors. While the majority of orthogonal arrays concentrate on primary effects, certain designs enable the assessment of particular interactions. Depending on the setup of the experiment, TD can either be used for screening or in-depth characterization and optimization. (Jankovic et al., 2021)

The Plackett-Burman design (PBD), created by J.P. Burman and R.L. Plackett, stands as one of the most widely used screening techniques for identifying the most important variables

among a multitude of others. By adapting PBD, information on the primary (first-order), impacts as well as two-factor interactions can be obtained, depending on the number of experimental runs. (Jankovic et al., 2021)

Definitive screening design (DSD) introduces a middle (third) level for continuous factors, while it reduces the necessary number of experimental runs. This is especially advantageous when a design is influenced by numerous factors. Simultaneously, the DSD is able to estimate two-factor interactions, even with a small number of experimental runs. It represents a good option for screening and is even potentially suitable for the characterization of complex problems that are influenced by a lot of factors. (Jankovic et al., 2021)

Box-Behnken design (BBD) and central composite design (CCD) are both designs associated with Response Surface Methodology and are oriented toward system optimization. In contrast to the beforementioned methods, these two may be used to assess higher-order terms (quadratic or cubic), while providing insight into the behavior of the system by showing a relationship between response and factors. Typically, CCD is used after performing certain screening methods to reduce the number of significant elements. In comparison to CCD, BBD requires fewer experimental runs and therefore has regions with lower prediction quality than CCD. As seen in the figure above, it lacks extreme points which might be particularly helpful for physical investigations where these points are occasionally costly and challenging to test. (Jankovic et al., 2021)

# Chapter 3

## Methodology

This chapter can be roughly divided into two sections. The first section deals with the numerical simulation of heat transport and mass flow within the aquifer, whereas the second section describes the DoE approach, where the output of 3.1 is used to further process the data.

### 3.1 Finite Element Flow Simulation

The subsurface ATEs simulations are conducted in FEFLOW (Finite Element subsurface FLOW and transport system). The software is a groundwater modeling system with various features like three-dimensional, transient, or steady state flow, mass and heat transport and many others. It can be used to model geothermal processes, estimate travel times of chemical species in aquifers, and plan and design remediation strategies. The training manual and introductory tutorial, as well as on-demand videos on how to set up a model are used to follow the according steps. After setting up a model and describing the problem, the data can be extracted and further processed in statistical programs or as .csv data. In total, 34 simulations are run to fulfill the requirements for the statistical analysis of the results of each case by using DoE.

#### 3.1.1 Numerical Model Setup

At the beginning of the model setup, the extension of the supermesh needs to be initialized. As there is no geological information available on the Vienna Basin, a conceptual box model is assumed. The 2D horizontal dimension of the aquifer is set to 1,500 m in x-direction which is parallel to the spacing of the well doublet and 1,000 m in y-direction, perpendicular to the gap of the injection and production well. The global coordinates of the origin of the local coordinate system are set to (0; 0) m, the position of Well 1 to (500; 500) m and Well 2 to (1,000; 500) m. Additionally, an inactive observation well is placed at the center of the well doublet at (750; 500) m. After using the concept of the ideal element size to minimize discretization effects around the well regarding concentration and temperature and proposing 10,000 elements for the model, it is expanded to a 3-dimensional model. E.g., for the base model simulation, the depth of the top of the aquifer is set to -1,550 m, with a thickness of 40 m and therefore an

elevation of -1,590 m for the bottom of the aquifer. For a better resolution of the results, the aquifer is split into 10 slices, corresponding to 9 layers and 100,000 elements in total. Additionally, impermeable layers are inserted above and below the aquifer which act as flow boundaries of the system in vertical direction. This way, the mass transport is prevented while still allowing the different formations to exchange thermal heat exchange via conduction. There are neither boundary conditions nor impermeable formations inserted in horizontal direction, as the model extension is large enough to prevent a breakthrough in any direction and no inflow nor outflow are defined. As for the BCs of the system, the pressure in the model is calculated automatically by FEFLOW, taking into consideration the depth and density of the liquid phase. In the simulations, a normally (hydrostatically) pressured zone is assumed for all cases. A multilayer well BC is applied in the systems along the whole length of the aquifer to simulate perforations along the entire formation and combined with a time-varying temperature BC to simulate the respective injection cycles. A snapshot of the model and its mesh is shown in Figure 9. The initial temperature of the system at  $t = 0$  d is set to 60 °C in the base case.

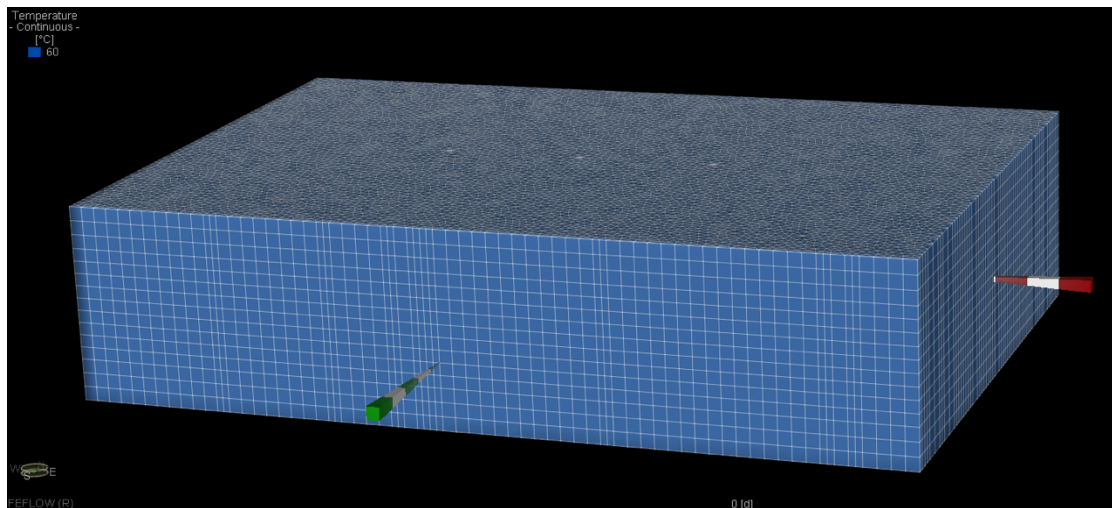


Figure 9: 3D view of the mesh model and the initial temperature of the system (created with FEFLOW)

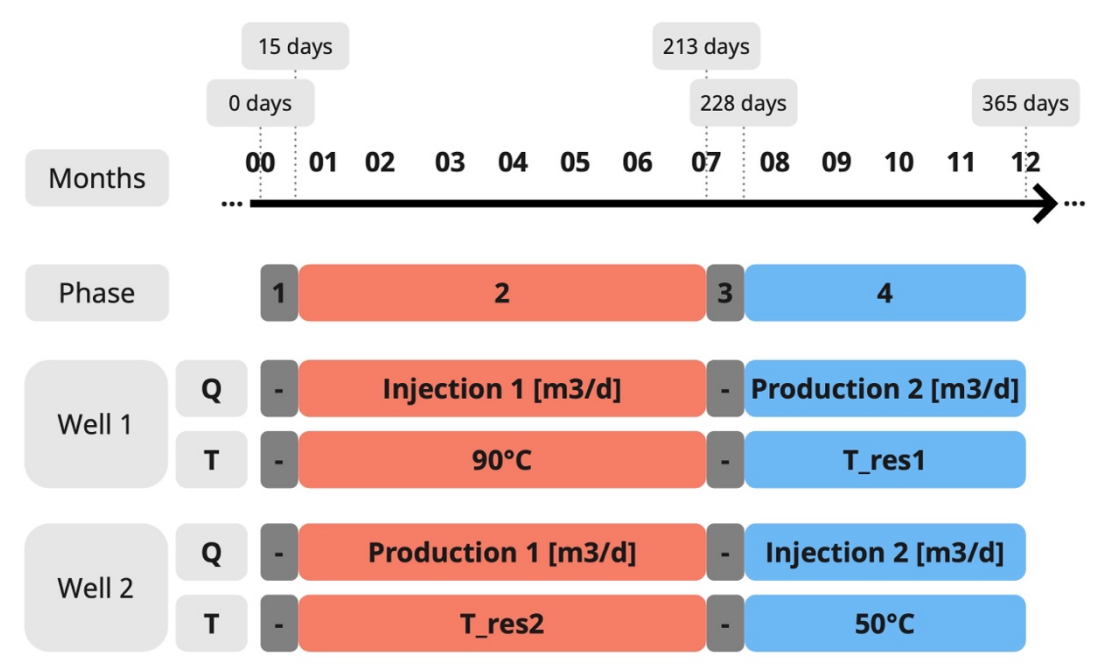


Figure 10: Overview of the four phases of each operating cycle (Created with Miro)

Figure 10 shows the four phases of a full operational cycle which takes 12 months to complete. Cycle 1 lasts for 15 days and is characterized by down-time of the whole system. Neither injection nor production are in place, so  $Q$  (flow rate) is equal to zero for Well 1 and Well 2 and the temperature boundary condition (BC) around the well is not active. In Phase 2 the heat injection begins. The temperature BC for Well 1 is set to  $90^{\circ}\text{C}$  and the injection rate is set to a fixed volume per day, depending on the case, but equals  $400,000\text{ m}^3$  over 198 days (6.5 months) during the base case. At the same time, Well 2 produces the volume that is injected into the conceptual model at the temperature that is present in the aquifer ( $T_{\text{res}2}$ ). After these six and a half months a propagation of heat around the injector can be observed. Again, in between reversing the flow direction of the system there is a down-time of 15 days with no injection/production and no temperature BC at both wells. This is followed by the fourth and last phase of the cycle, where the previous injector becomes the producer and vice versa. Well 1 produces hot fluid that has accumulated around the well at a dynamic temperature profile that results from heat transfer and fluid flow in the aquifer. By setting the temperature BC of Well 2 to  $50^{\circ}\text{C}$ , an assumption is made that the temperature difference between the produced and injected temperature, minus its losses, is used in a heat exchanger at the surface for a DHN. The flow rate over 137 days is again  $400,000\text{ m}^3$  for this phase. This whole cycle is then repeated for a continuous four years, while the temperature BCs and the flow rates are assumed to be the same over the whole lifetime of the system.

The parameters that do not change over the different cases and are important to consider in HT-ATES are listed in the following table.

Parameter	Value	Unit
Anisotropy of Solid Heat Conductivity	1	[-]
Heat conductivity fluid	0.65	[W/m/K]
Heat conductivity solid	3	[W/m/K]
Dispersivity longitudinal	5	[m]
Dispersivity transverse	0.5	[m]
Volumetric heat capacity fluid	4.2E+6	[J/m <sup>3</sup> /K]
Volumetric heat capacity solid	2.52E+6	[J/m <sup>3</sup> /K]
Anisotropy of Conductivity/Transmissivity	1	[-]

Table 2: Fixed parameters in the numerical simulation

These parameters that are subject to change and are further investigated in the workflow are hydraulic conductivity, porosity, injection rate, aquifer thickness, specific fluid gravity, groundwater flow and aquifer temperature. Their minimum, medium (most likely) and maximum values are given in the next table.

Parameter	Min	Med	Max	Unit
Hydraulic Conductivity	0.1	1	10	[m/d]
Porosity	8	15	25	[-]
Injection Rate	300,000	400,000	500,000	[m <sup>3</sup> /y]
Aquifer Thickness	15	40	100	[m]
Specific Fluid Gravity	1	1.075	1.5	[-]
Groundwater Flow		0	1	[m/y]
Aquifer Temperature	40	60	80	[°C]

Table 3: Variable parameters in the numerical simulation

### 3.1.2 Base Model

All the input data for the various models can be obtained from the simulation matrix in 3.1.1. This section is used to describe the base model in more detail. After consultation with a geologist based around the Vienna Basin, the parameters that have been set are considered realistic and to be expected in aquifers there. The simulation is conducted according to the setup that has been described in the previous chapter and further analyzed to obtain the thermal recovery efficiency of the system.

Figure 11 shows the course of temperature of the two wells that are placed in the aquifer. The upper, blue line (a) represents Well 1, also known as the hot well and the lower, red line (b) displays Well 2, the cold well of the system. The sections of each temperature distributions that are perfectly horizontal demonstrate the injection of brine at the pre-defined BC at the respective well, while the sections of large variation of temperature over time demonstrate the production phase of each well. As the aquifer temperature is set to 60°C, and the injection temperatures of Well1 and Well 2 are 90°C and 50°C, respectively, the aquifer is heated up and cooled down at different locations.

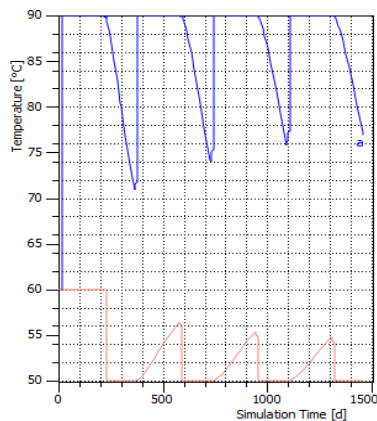


Figure 11: Course of temperature over 1460 days for Well 1 and Well 2 (Created with FEFLOW)

With each year, the temperature around the hot well (left hand side) is increasing, ranging from 70.85 °C to 76.98 °C for cycle one and cycle four, respectively. This can be attributed to the fact that heat is stored in the system around the well from each cycle. Ultimately, this results in an increased efficiency of ATEs over time, as the return temperatures increase with constant injection and production temperatures and rates over the years.

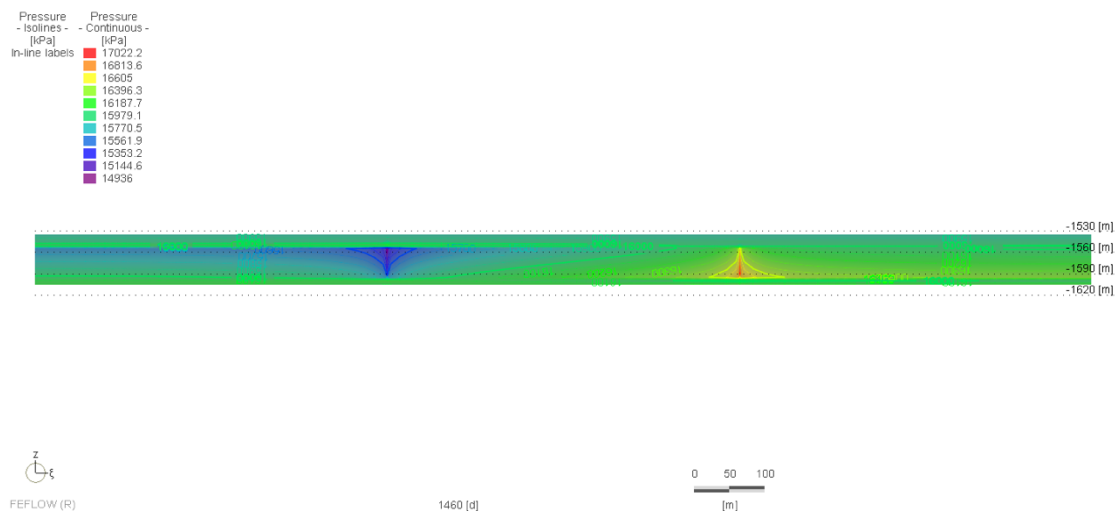


Figure 12: Pressure distribution in the base case at 1460 days (Created with FEFLOW)



Figure 12 shows the pressure distribution within the system at 1460 days. This moment represents the end of Phase 4 (heating period), Cycle 4. On the right side of the hot well the hydraulic influence of the cold well can be seen, as the pressure is influenced by the simultaneous production at Well 2. There is almost no influence in the upper and lower part of the graph which is because these regions are cut off by an impermeable layer (no flow BC) as described above.

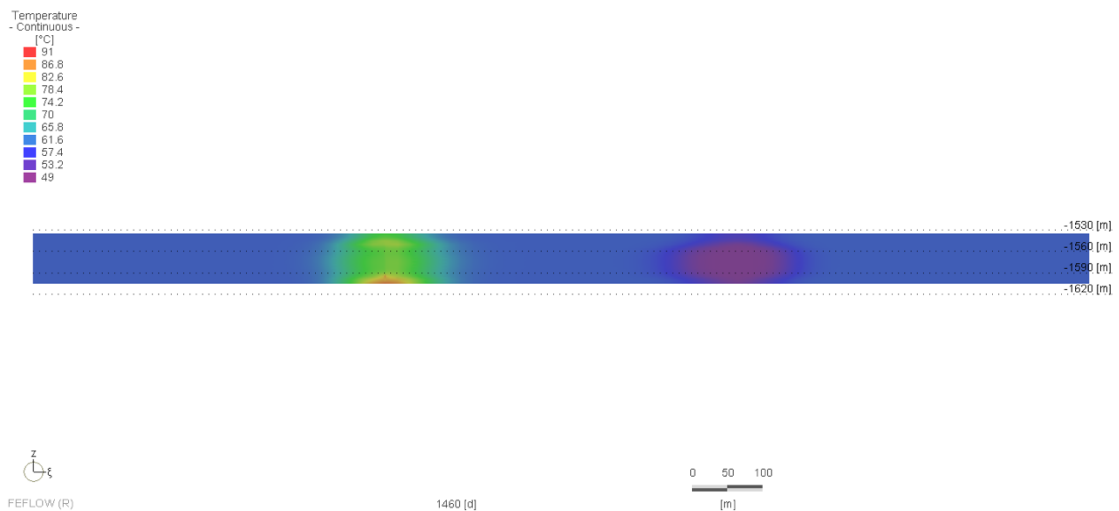


Figure 13: Temperature distribution in the base case at 1460 days (Created with FEFLOW)

Figure 13 shows the temperature distribution at 1460 days, the same time step as in Figure 12. In contrast to the undisturbed pressure regime in the impermeable region, the layers experience a change in temperature over time. This is caused by conductive heat transfer, as described in the literature review.

### 3.2 Design of Experiments Approach

As the parameters that influence the thermal recovery efficiency of HT-ATES are numerous, a thorough and well considered approach is necessary to obtain not only the influence of each variable individually but also their interaction. Therefore, a DoE approach is chosen to evaluate the optimization of the system. As indicated in the literature review, there are various ways on how to conduct DoE. In this thesis, a pre-selection of parameters that are considered as fixed is set in Table 2. The next step is to identify the heavy hitters of the parameters that undergo a change from minimum to maximum levels, otherwise the total number of simulations would be not feasible to conduct because of computational time. Even though one factor at a time (OFAT) as a screening method is not always considered the most effective, it was used due to its easy set up for screening. The total number of simulations was 14 including the base case for the screening. The thermal recovery efficiency as the response value of each case was compared to see the effect that the minimum and maximum values have on the outcome. The results for the

screening are shown in the next chapter. After identifying the most influencing parameters, a FFD was used to not only describe the main effects of each parameter but also the interaction between them. For this, the commercial software DATAtab was used. The online-tool not only helps with the numerical results and graphical illustration, but it also uses AI-interpretation of the results to help understand the findings. The results are again shown in the next chapter.

Case	Thickness	Injection Rate	Conductivity
1	Low	Low	Low
2	Low	Low	Base
3	Low	Low	High
4	Low	Base	Low
5	Low	Base	Base
6	Low	Base	High
7	Low	High	Low
8	Low	High	Base
9	Low	High	High
10	Base	Low	Low
11	Base	Low	Base
12	Base	Low	High
13	Base	Base	Low
14	Base	Base	Base
15	Base	Base	High
16	Base	High	Low
17	Base	High	Base
18	Base	High	High
19	High	Low	Low
20	High	Low	Base
21	High	Low	High
22	High	Base	Low
23	High	Base	Base
24	High	Base	High
25	High	High	Low
26	High	High	Base
27	High	High	High

*Table 4: FFD simulation matrix*

The table above shows the simulation matrix for the FFD. Each factor is changed to its low, base, and high case to follow the methodology accordingly.

# Chapter 4

## Results and Discussion

The recovery efficiency of the base case simulation is considered the reference value for the following analysis and is determined as 72.03 %. Figure 14 shows a 2D slice view in 1570 m depth after the full operational time of 1460 days. No thermal breakthrough is observed after four years of operation and the mean temperature at the hot well is 76.98 °C.

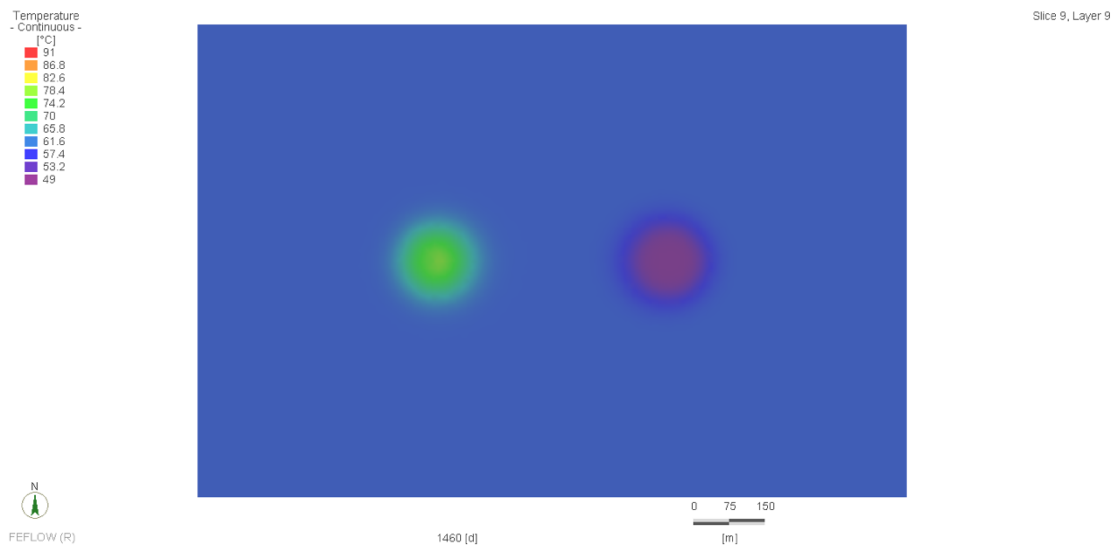


Figure 14: Bird's-eye view of the temperature distribution in the system on slice 9 at 1460 days

In this case,  $2.17\text{E}+11$  J of heat are injected into the aquifer and  $1.56\text{E}+11$  J are recovered after four years. The next step in the workflow was to identify the heavy hitters to reduce the number of parameters that are investigated to influence the recovery efficiency. As indicated in the previous chapter, OFAT analysis was applied. The individual impacts of the minimum and maximum value of each input variable were summed up to get the total amount of change that the system experiences and the effect of each variable was investigated.

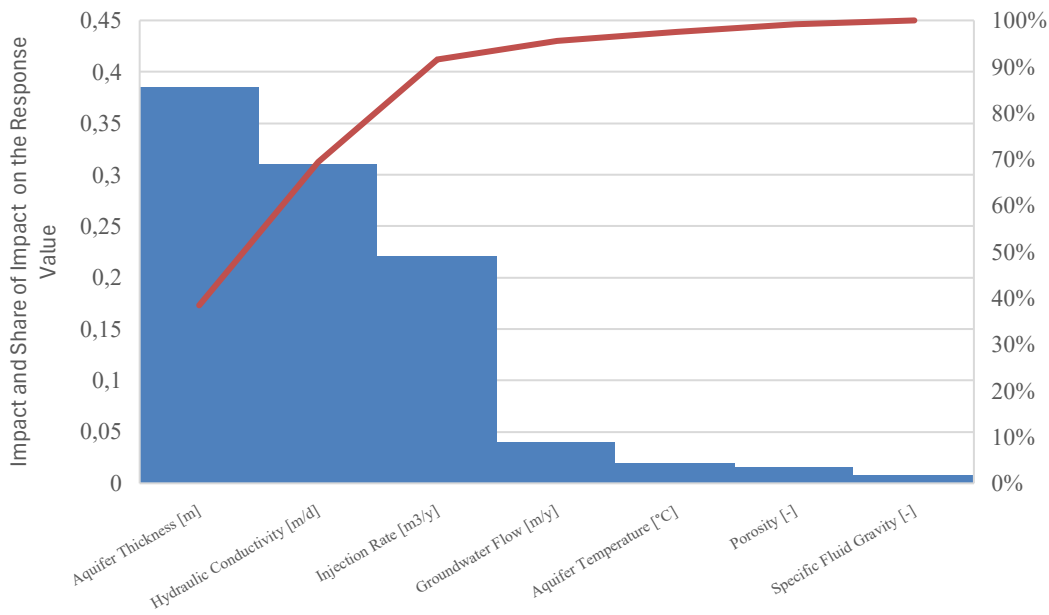


Figure 15: Pareto diagram for the OFAT analysis

Figure 15 shows that the main impact on the thermal recovery efficiency is induced by aquifer thickness, hydraulic conductivity, and injection rate. Groundwater flow, aquifer temperature, porosity, and specific fluid gravity combined contribute to less than 10 % of the total deviation from the base case and are therefore excluded from the next steps of the analysis.

At this moment it is important to note that the total amount of heat produced in the case of a higher ambient aquifer temperature is much higher, however, the thermal recovery efficiency does not change by a lot. Groundwater flow is considered to be an important parameter in ATES efficiency, in this case the magnitude of 1 m/y is too less to have an overwhelming impact. In shallow aquifers where groundwater flow can reach multiples of this value, this parameter needs special focus.

The three main influencing parameters (factors) were used to conduct a FFD on three levels. The according simulation matrix is already shown in the previous chapter. With 75.00 % the combination of base thickness, high injection rate and low conductivity yielded the highest recovery efficiency. The lowest efficiency of 65.36 % is yielded for high thickness, low injection rate, and high conductivity.

A requirements test was conducted to test the normal distribution of residuals.

	Statistics	p
Kolmogorov-Smirnov	0,1	0,907
Kolmogorov-Smirnov (Corr. Lilliefors)	0,1	0,661
Shapiro-Wilk	0,96	0,287
Anderson-Darling	0,37	0,429

Table 5: Four tests for the normal distribution of the residuals (Created with DATAtab)

A high p-value ( $> 0.05$ ) indicates that the data does not deviate significantly from the normal distribution which is the case for all four tests. This allows for continuing with statistical methods.

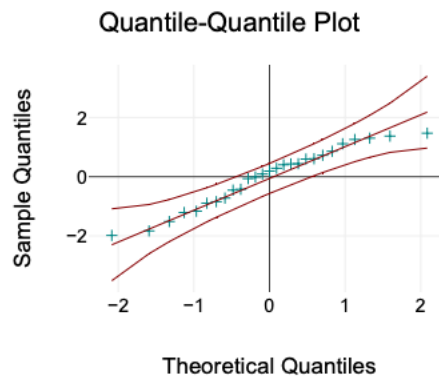


Figure 16: Q-Q plot for the results (Created with DATAtab)

Figure 17 shows the main effects of the three factors at their three levels, while Figure 18 shows the interaction of each of the input factors. While for both, an increase in injection rate and a decrease in conductivity the recovery efficiency increases, the effect of the thickness shows a more complex course. Low and high thickness both lead to a decrease of the performance in comparison to the base case. This is according to the literature review, where low to medium thick aquifers are considered more efficient than high thickness aquifers. There seems to be a trade-off between conductive heat losses that dominate in thinner aquifers and convective heat losses that are increasingly important to consider in thicker aquifers. The decrease in hydraulic conductivity limits this buoyancy-driven flow which results in less heat losses, as the conductivity

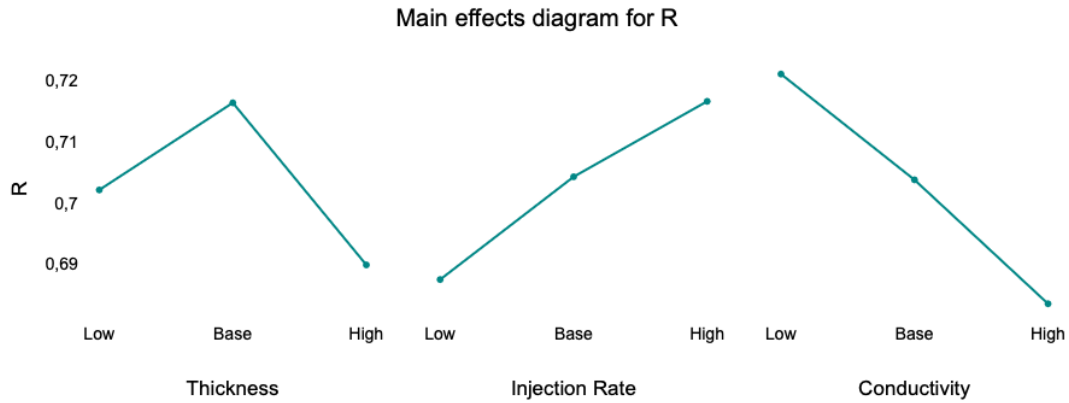


Figure 17: Influence of main effects on the system performance (Created with DATAtab)

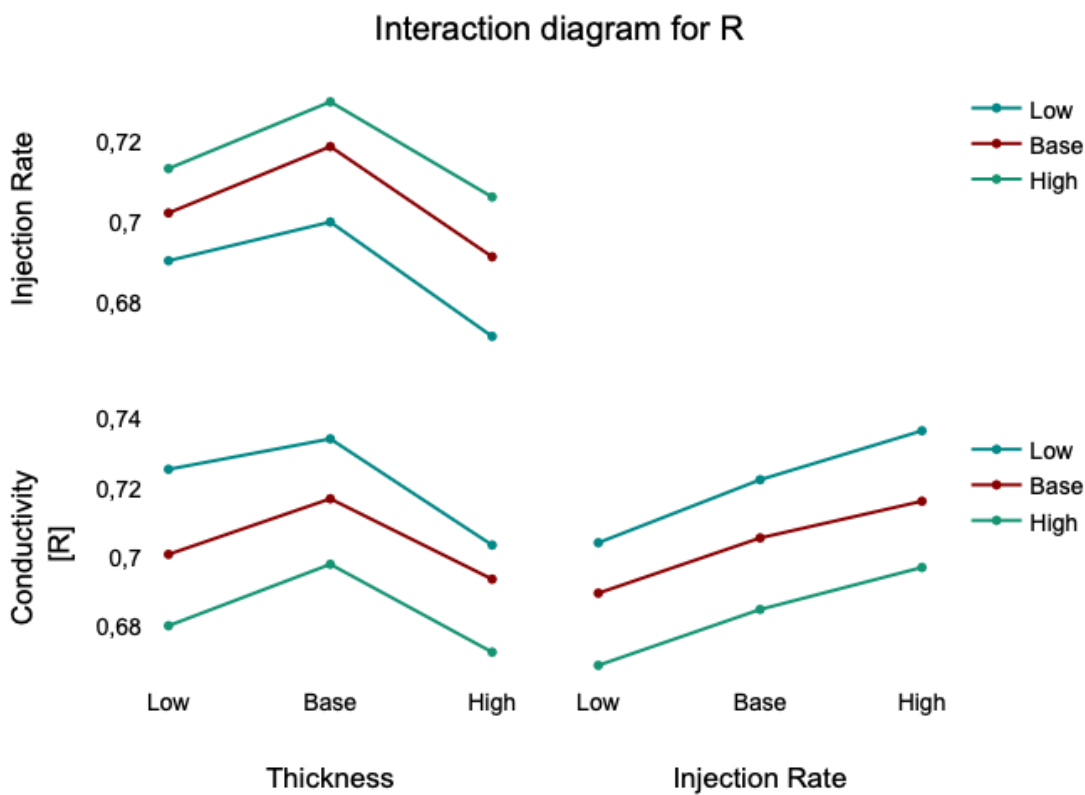


Figure 18: Influence of interaction effects on the system performance (Created with DATAtab)

Regardless of the values of conductivity and thickness, a higher injection rate always results in a higher thermal recovery efficiency. Also, lower hydraulic conductivity leads to a higher R than the base and low case. With thickness, this trend cannot be observed. The base thickness yields the best performance out of the three values that range between 15 m, 40 m, and 100 m.

The table below shows the results for the ANOVA that was created with DATAtab. It includes degrees of freedom, adjusted sum of squares, adjusted mean squares, and the F- and p-value for the main effects and interaction effects.

	df	Adj SS	Adj MS	F	p
Model	18	0,01	0	295,58	<0,001
Thickness	2	0	0	613,33	<0,001
Injection Rate	2	0	0	745,77	<0,001
Conductivity	2	0,01	0	1231,45	<0,001
Thickness*Injection Rate	4	0	0	11,27	0,002
Thickness*Conductivity	4	0	0	20,91	<0,001
Injection Rate*Conductivity	4	0	0	2,64	0,113
Error	8	0	0		

Table 6: ANOVA results for the FFD (created with DATAtab)

It seems that the main effects have a higher influence on the performance of the system than the interaction effects. The model also seems to be fitted, a multiple linear regression was conducted and variable  $R^2 = 0.97$  was calculated by DATAtab.

	$f^2$
Thickness Low	8,44
Thickness High	11,2
Injection Rate Low	12,84
Injection Rate High	14,19
Conductivity Low	17,71
Conductivity High	18,44

Table 7: Cohens  $f^2$  for the variables compared to the base value (Created with DATAtab)

Furthermore, Cohens  $f^2$  was assessed to describe the effect size each variable has on the base case. In the range of parameters that were assessed, conductivity has the strongest influence. This might be due to the larger range of the input parameter.





# Chapter 5

## Conclusion

This thesis has focused on the design and optimization of HT-ATES in the Vienna basin, while a special focus lies on the aquifer component. After identifying the most influencing parameters of the system, they have been estimated to be consistent with the local geology of the area. Through a total of 34 simulations the impact of the relevant parameters was obtained via numerical simulations in FEFLOW. By following the methodology of DoE with a screening method that was followed by a FFD, the individual influence and their interaction effects are demonstrated in this thesis. Furthermore, pressure and temperature profiles in a confined aquifer are shown to understand the thermal and hydraulic behavior of the system. However, the current state of knowledge on HT-ATES is very limited. Only a small number of real-world implementations are in operation and long-time studies are not yet too informative. The range of parameters is very limited, as the simulations are only focused on the Vienna Basin. A larger approach might be necessary to assess, where and under what circumstances the implementation of HT-ATES is a valid contribution to the local energy efficiency improvements. Aquifer thickness, injection rate, and hydraulic conductivity have been identified to have the most powerful impact on the performance of the system. The combination of a medium-thick aquifer, low hydraulic conductivity and high injection rate is determined to be the best combination of parameters. As for the future work in this field, a holistic approach is suggested to not only assess the aquifer of the system itself but to combine it with heating demand, production facilities, and heating supply. Additionally, geochemical and biological reactions within the aquifer might lead to operational difficulties that have not been addressed here. This is another focus, future work should aim to tackle.



## References

- Aydin Ertuğrul, N., HatiPoğlu Bağci, Z., & Ertuğrul, Ö. L. (2018). AQUIFER THERMAL ENERGY STORAGE SYSTEMS: BASIC CONCEPTS AND GENERAL DESIGN METHODS. *Turkish Journal of Engineering*, 2(2), 38–48. <https://doi.org/10.31127/tuje.340334>
- Beernink, S., Hartog, N., Vardon, P. J., & Bloemendal, M. (2024). Heat losses in ATEs systems: The impact of processes, storage geometry and temperature. *Geothermics*, 117, 102889. <https://doi.org/10.1016/j.geothermics.2023.102889>
- Birdsell, D. T., Adams, B. M., & Saar, M. O. (2021). Minimum transmissivity and optimal well spacing and flow rate for high-temperature aquifer thermal energy storage. *Applied Energy*, 289, 116658. <https://doi.org/10.1016/j.apenergy.2021.116658>
- Bloemendal, M., & Hartog, N. (2018). Analysis of the impact of storage conditions on the thermal recovery efficiency of low-temperature ATEs systems. *Geothermics*, 71, 306–319. <https://doi.org/10.1016/j.geothermics.2017.10.009>
- COP28: *Global Renewables And Energy Efficiency Pledge*. (n.d.). Retrieved 24 March 2024, from <https://www.cop28.com/en/global-renewables-and-energy-efficiency-pledge>
- Daniilidis, A., Mindel, J. E., De Oliveira Filho, F., & Guglielmetti, L. (2022). Techno-economic assessment and operational CO<sub>2</sub> emissions of High-Temperature Aquifer Thermal Energy Storage (HT-ATES) using demand-driven and subsurface-constrained dimensioning. *Energy*, 249, 123682. <https://doi.org/10.1016/j.energy.2022.123682>

- Fleuchaus, P., Godschalk, B., Stober, I., & Blum, P. (2018). Worldwide application of aquifer thermal energy storage – A review. *Renewable and Sustainable Energy Reviews*, *94*, 861–876. <https://doi.org/10.1016/j.rser.2018.06.057>
- Gao, L., Zhao, J., An, Q., Wang, J., & Liu, X. (2017). A review on system performance studies of aquifer thermal energy storage. *Energy Procedia*, *142*, 3537–3545. <https://doi.org/10.1016/j.egypro.2017.12.242>
- García Gil, A., Garrido Schneider, E. A., Mejías Moreno, M., & Santamarta Cerezal, J. C. (2022). *Shallow Geothermal Energy: Theory and Application*. Springer International Publishing. <https://doi.org/10.1007/978-3-030-92258-0>
- Gunst, R. F., & Mason, R. L. (2009). Fractional factorial design. *WIREs Computational Statistics*, *1*(2), 234–244. <https://doi.org/10.1002/wics.27>
- Hartog, N., Drijver, B., Dinkla, I., & Bonte, M. (2013). *Field assessment of the impacts of Aquifer Thermal Energy Storage (ATES) systems on chemical and microbial groundwater composition*.
- Jankovic, A., Chaudhary, G., & Goia, F. (2021). Designing the design of experiments (DOE) – An investigation on the influence of different factorial designs on the characterization of complex systems. *Energy and Buildings*, *250*, 111298. <https://doi.org/10.1016/j.enbuild.2021.111298>
- Kallesøe, A. J., & Vangkilde-Pedersen, T. (2019). *Underground Thermal Energy Storage (UTES) – state-of-the-art, example cases and lessons learned*.
- Kleyböcker, A., & Bloemendal, M. (2020). *Factsheet – Aquifer thermal energy storage (ATES)*.
- Kuang, X., Jiao, J. J., Zheng, C., Cherry, J. A., & Li, H. (2020). A review of specific storage in aquifers. *Journal of Hydrology*, *581*, 124383. <https://doi.org/10.1016/j.jhydrol.2019.124383>
- Lu, H., Tian, P., Guan, Y., & Yu, S. (2019). Integrated suitability, vulnerability and sustainability indicators for assessing the global potential of aquifer thermal energy storage. *Applied Energy*, *239*, 747–756. <https://doi.org/10.1016/j.apenergy.2019.01.144>
- Mangold, D., Schmidt, T., & Müller-Steinhagen, H. (2004). Seasonal Thermal Energy Storage in Germany. *Structural Engineering International*, *14*(3), 230–232. <https://doi.org/10.2749/101686604777963739>
- Nielsen, J. E., & Vangkilde-Pedersen, T. (2019). *Underground Thermal Energy Storage (UTES) – general specifications and design*. [https://www.heatstore.eu/documents/HEATSTORE\\_WP1\\_D1.2\\_Final\\_v2019.09.20.pdf](https://www.heatstore.eu/documents/HEATSTORE_WP1_D1.2_Final_v2019.09.20.pdf)

- 
- Nitschke, F., Ystroem, L., Bauer, F., & Kohl, T. (n.d.). *Geochemical Constraints on the Operations of High Temperature Aquifer Energy Storage (HT-ATES) in Abandoned Oil Reservoirs*.
- Possemiers, M., Huysmans, M., & Batelaan, O. (2014). Influence of Aquifer Thermal Energy Storage on groundwater quality: A review illustrated by seven case studies from Belgium. *Journal of Hydrology: Regional Studies*, 2, 20–34. <https://doi.org/10.1016/j.ejrh.2014.08.001>
- Schmidt, T., Pauschinger, T., Sørensen, P. A., Snijders, A., Djebbar, R., Boulter, R., & Thornton, J. (2018). Design Aspects for Large-scale Pit and Aquifer Thermal Energy Storage for District Heating and Cooling. *Energy Procedia*, 149, 585–594. <https://doi.org/10.1016/j.egypro.2018.08.223>
- Sheldon, H. A., Wilkins, A., & Green, C. P. (2021). Recovery efficiency in high-temperature aquifer thermal energy storage systems. *Geothermics*, 96, 102173. <https://doi.org/10.1016/j.geothermics.2021.102173>
- Telford, J. K. (2007). A Brief Introduction to Design of Experiments. *Johns Hopkins APL Technical Digest*, 27(3).
- World Energy Outlook 2023*. (n.d.).
- Xiang, Y., Xie, Z., Furbo, S., Wang, D., Gao, M., & Fan, J. (2022). A comprehensive review on pit thermal energy storage: Technical elements, numerical approaches and recent applications. *Journal of Energy Storage*, 55, 105716. <https://doi.org/10.1016/j.est.2022.105716>



# Appendix

Case	Thickness	Injection Rate	Conductivity	R
1	Low	Low	Low	71,06%
2	Low	Low	Base	69,00%
3	Low	Low	High	67,08%
4	Low	Base	Low	72,61%
5	Low	Base	Base	70,11%
6	Low	Base	High	67,98%
7	Low	High	Low	73,94%
8	Low	High	Base	71,11%
9	Low	High	High	68,96%
10	Base	Low	Low	71,65%
11	Base	Low	Base	70,23%
12	Base	Low	High	68,15%
13	Base	Base	Low	73,60%
14	Base	Base	Base	72,03%
15	Base	Base	High	70,02%
16	Base	High	Low	75,00%
17	Base	High	Base	72,79%
18	Base	High	High	71,19%
19	High	Low	Low	68,52%
20	High	Low	Base	67,62%
21	High	Low	High	65,36%
22	High	Base	Low	70,49%
23	High	Base	Base	69,51%
24	High	Base	High	67,44%
25	High	High	Low	72,02%
26	High	High	Base	70,94%
27	High	High	High	68,93%

Tab. 1: Thermal recovery efficiency for each case of the FFD





# List of Figures

Figure 1: BTES conceptual model. (a) cross-sectional view of the system (b) model of the whole system in combination with DHN (c) borehole array from a bird's-eye view (Gao et al., 2023) .....	14
Figure 2: PTES. Real image in bird's-eye view and a conceptual cross-sectional view (Xiang et al., 2022) .....	15
Figure 3: MTES. Operating cycle in summer and winter (Kallesøe & Vangkilde-Pedersen, 2019).....	15
Figure 4: Achievements in the history of ATES projects from 1960 until 2020 (Fleuchaus et al., 2018).....	17
Figure 5: Global potential of ATES on a global scale (Lu et al., 2019).....	18
Figure 6: Well doublet and star-shaped configuration (Nielsen & Vangkilde-Pedersen, 2019) .....	20
Figure 7: Heat losses in HT-ATES (Beernink et al., 2024).....	23
Figure 8: Various DoE for a three factor model on five levels (Jankovic et al., 2021).....	26
Figure 9: 3D view of the mesh model and the initial temperature of the system (created with FEFLOW).....	29
Figure 10: Overview of the four phases of each operating cycle (Created with Miro).....	30
Figure 11: Course of temperature over 1460 days for Well 1 and Well 2 (Created with FEFLOW).....	32
Figure 12: Pressure distribution in the base case at 1460 days (Created with FEFLOW) .....	32
Figure 13: Temperature distribution in the base case at 1460 days (Created with FEFLOW) .....	33
Figure 14: Bird's-eye view of the temperature distribution in the system on slice 9 at 1460 days .....	35
Figure 15: Pareto diagram for the OFAT analysis .....	36
Figure 16: Q-Q plot for the results (Created with DATAtab) .....	37
Figure 17: Influence of main effects on the system performance (Created with DATAtab) ...	38
Figure 18: Influence of interaction effects on the system performance (Created with DATAtab) .....	38

## List of Tables

Table 1: Relevant aquifer parameters in ATES (Kallesøe & Vangkilde-Pedersen, 2019).....	21
Table 2: Fixed parameters in the numerical simulation.....	31
Table 3: Variable parameters in the numerical simulation.....	31
Table 4: FFD simulation matrix .....	34
Table 5: Four tests for the normal distribution of the residuals (Created with DATAtab) .....	37
Table 6: ANOVA results for the FFD (created with DATAtab).....	39
Table 7: Cohens $f^2$ for the variables compared to the base value (Created with DATAtab)....	39



# Abbreviations

AI	Artificial intelligence
ATES	Aquifer thermal energy storage
BBD	Box-Behnken design
BC	Boundary condition
BHE	Borehole heat exchangers
BTES	Borehole thermal energy storage
CCD	Central composite design
CHP	Combined heat and power
COP	Conference of the Parties
DHN	District heating network
DoE	Design of experiments
DSD	Definitive screening design
ECES	Energy Conservation through Energy Storage
FFD	Full factorial design
HT-ATES	High-Temperature aquifer thermal energy storage
IEA	International Energy Agency
LCOH	Levelized cost of heat
LT-ATES	Low-Temperature aquifer thermal energy storage
MT-ATES	Medium-Temperature aquifer thermal energy storage
MTES	mine thermal energy storage
OFAT	One factor at a time
PBD	Plackett-Burman design
PTES	Pit thermal energy storage
R&D	Research and development
TES	Thermal energy storage
TG	Taguchi design

UTES                      Underground thermal energy storage